

# Contrast Enhancement of Satellite Images Using Dual- Tree Complex Wavelet Transforms Technique

<sup>[1]</sup> M.Hemalatha <sup>[2]</sup>Dr.S.Varadarajan <sup>[3]</sup>A.V.Kiranmai  
<sup>[1]</sup>Research Scholar <sup>[2]</sup> Professor <sup>[3]</sup> Assistant Professor  
<sup>[1][2][3]</sup>Department of ECE, Sri Venkateswara University, Tirupathi

**Abstract:**—this paper forwards enhancement of satellite picture using Discrete Time Complex Wavelet Transform Technique. The discrete-wavelet-transform-based (DWT) contrast image scheme generates artifacts (due to a DWT shift-variant property). A wavelet-domain approach based on dual-tree complex wavelet transform (DT-CWT) proposed for contrast of the satellite images. A satellite input image is decomposed by DT-CWT (which is nearly shift invariant) to obtain high-frequency subbands. The high-frequency subbands and the low-resolution (LR) input image are interpolated using the Lanczos interpolator. The high-frequency subbands are passed through an NLM filter to cater for the artifacts generated by DT-CWT (despite of its nearly shift invariance). The filtered high-frequency subbands and the LR input image are combined using inverse DT-CWT to obtain a resolution-enhanced image. The contrast enhancement method uses the analysis of excellent glaze levels and appropriate flexible radiant transfiguration which performs DWT in reducing the rate of image which is given as input, into a group of band bounded constituents by a sampling factor, called High-High, High-Low, Low-High, and Low-Low sub bands. The brightness propaganda is contained in the Low-Low sub-band where the input image with the superlative glaze level is computed. According to the superlative glaze level the Low-Low sub band is disintegrated into trilayer. The suitable flexible radiant transfiguration is processed in the disintegrated trilayer of the sub-band using knee shift function, dominant glaze level and gamma adjustment function. For preserving the texture of contrast suitable enhanced flexible radiant transfiguration is processed. The final enhanced image is acquired by means of the use of inverse DWT. In this method, the distant sensed image is bifurcated into petite blocks, and then each block is improvised using advanced block based discrete wavelet transform. The enhanced blocks are then fused together and by using inverse DWT, the emanated image is obtained. The glaze and radiance of the satellite image will be better when compared with the image used in the Existing systems. Haar Wavelet Transform (HWT) is used for disintegrating the pictures into sub-bands. Trilayer is formed using preeminent glaze level analysis. From the preeminent glaze, each disintegrated layer there is a generation of suitable radiance transfer function.

**Keywords:** -- Complex Wavelet Transform, Discrete wavelet transform (DWT), Preeminent glaze level analysis, Flexible radiant transfiguration.

## I. INTRODUCTION

Image processing is the processing of an input image by means of numerous varieties of modus and computative processing devices. A picture usually undergoes some form of basic improvising steps, for the beneficial of filtering the segmenting of interesting data and to descend other data [1].

A digital portrait is indicated by means of a multitude with completely spaced and very little limited samples of the image. double process that are very similar to most of the digital systems are selection and limitation. When a picture is discredited, it is indicated in flatly spaced samples. These limited samples are called as pixels. To indicate a normal monochrome television portrait digitally, a multitude of  $512 \times 512$  pixels is necessary. Every part of

pixels in a portrait is entitled by an eight bit number for allowing 256 grey levels. Therefore an individual monochrome television portrait requires about  $2 \times 10^6$  bits. For isolated sensing images the authors in [2] and [3] explained a detailed contrast enhancement technique by edge detection and histogram equalization methods. In [17] Ankit Aggarwal, R.S. Chauhan and Kamaljeet Kaur approach a method for defining the connection between a numerical value of pixel and its actual luminance. It is also referred to as gamma correction. Types of gamma correction are Image gamma, Display gamma and System gamma. Image Gamma is applied either by RAW development software or by a camera whenever an image is captured it is converted into a standard JPEG or TIFF file. The main purpose of the display gamma is to recover for a file's gamma thereby making sure that the image is not unrealistically brightened when it is displayed onto the screen. System Gamma represents the overall net effect of

**International Journal of Engineering Research in Electronics and Communication  
Engineering (IJERECE)  
Vol 3, Issue 10, October 2016**

all gamma values that have been applied to an image, and is also mentioned as the "viewing gamma". For authentic replication of a scene, this should be close to a straight line (gamma = 1.0), but, the system gamma is sometimes slightly greater than 1.0 in order for improving the contrast [6-9]. Enhancement comprises of improvising the variance, deleting computational aberration, softening the contours, or modifying of the portrait in order to facilitate the perception of its message content. In [10] Hasanul Kabir, Abdullah Al-Wadud, and Oksam Chae, explains about radiance stabilizing transfiguration using weighted mixture of overall and regional transfigurations. Similarly [11] Akhilesh Verma, Archana describes the survey based on image contrast enhancement by using genetic algorithm. By using discrete wavelet transform (DWT) and singular value decomposition Hasan Demirel, Cagri Ozcinar, and Gholamreza Anbarjafar approaches a contrast based enhancement for only satellite images [7].

## II HAAR WAVELET TRANSFORM

The basic wavelet transform using 2-D wavelet decomposition is shown in Fig.1. The decomposition obtained from DWT is of four sub-bands namely Low-Low, Low-High, High-Low and High-High. The divided bands frequency components overlay the full-frequency spectrum of the real image. The Low-Low sub-band has the information content of the image. It is achieved by low pass refining of the portrait [11-14]. All the other sub-bands is used to provide high frequency component i.e. edges. Consider the input image of size 512 x 512 as shown in Fig .2

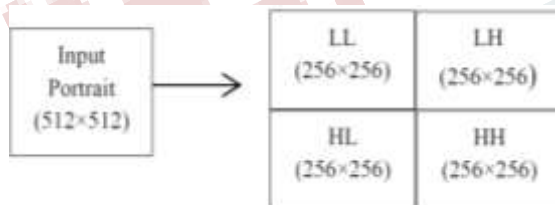


*Fig.1. Size of Sub-Bands after Decomposition*

## III. BLOCKBASED CONTRAST ENHANCEMENT TECHNIQUE

The Low-Low sub-band contains the approximate details of the original portrait and the other triple sub-bands consist of the contour details of the portrait. The Low-Low sub band which has the overall approximate details are processed using preeminent glaze level method and suitable radiant transfiguration.

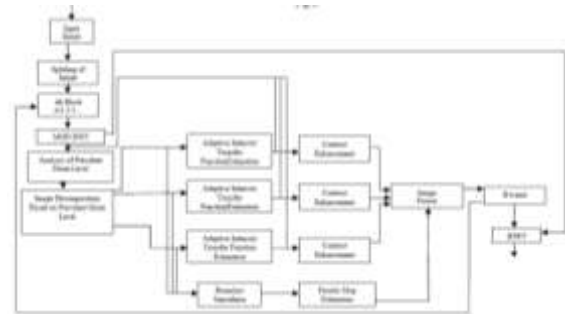


*Fig.2. Block Based Contrast Enhancement Using DWT*

The preeminent glaze level analysis is used in the formation of trilateral namely low radiant, middle radiant and high radiant layers [15]. Fig.2. elucidates the block diagram of the block based modified DWT portrait radiance improvising method

### A. Discrete Wavelet Transform

The basic concept of the DWT is to sector the portrait into low and high sub bands. The Low sub band and high sub band are used to form LL, LH, HL and HH. The diagrammatic representation of the DWT is given in the Fig .4.

### B. Wavelet Function and Algorithm

Wavelet algorithms are repetitive. The resultant of one process of the algorithm becomes the entry for the next process. The first entry data group constitute of  $2n$  parts. Each repeated step works on  $2n-i$  parts, where  $i = 1 \dots n-1$ . For instance, if the initiative data group comprise 128 parts, the wavelet conversion will be constituted of 7 steps on 128, 64, 32, 16, 8, 4, and 2 units. The dataset being processed gets divided into a flat division and a peculiar division by using progressive arising device wavelet conversion. The algorithm which is proposed is explained in flow chart as shown in Fig.3.

**International Journal of Engineering Research in Electronics and Communication  
Engineering (IJERECE)  
Vol 3, Issue 10, October 2016**

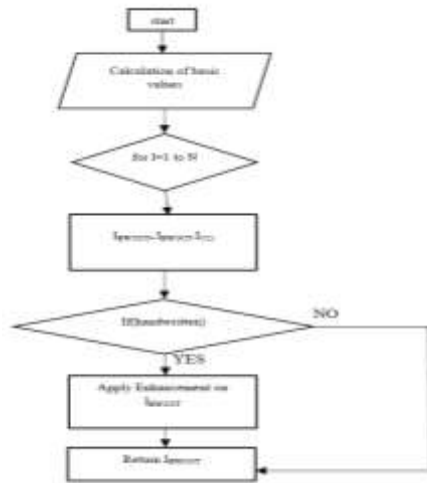


**Fig.3. Flow chart for algorithm**

**C. Update Step:** The update step restores the flat divisions with a median. These outcomes a flatter input for the successive step of the wavelet conversion. The peculiar divisions also indicate an estimation of the native data group, allowing filters to be created. Fig.5. provides an easy progressive arising conversion block diagram. Finally the images are merged together and inverse DWT is utilized to obtain the final improved image.

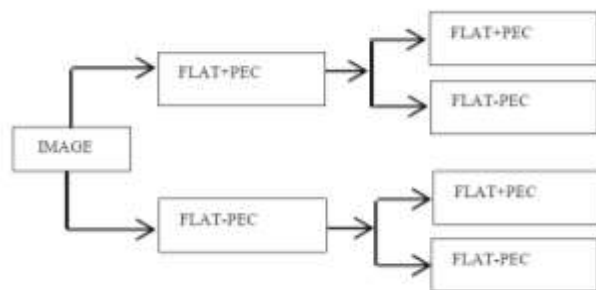


**Fig.4. Block Diagram of DWT**

The variations that are stored in the irregular units must be operated with the median update phase that is given by Equation 1.

$$Flat_{j+1,i} = flat_{j,i} + U(pec_{j+1,i}) \quad (1)$$

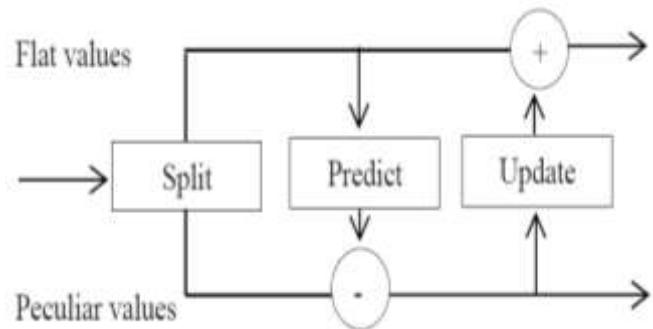


**Fig.5. Progressive Arising Conversion**

In arising device form of HAAR transform, the detection step identifies that the peculiar divisions will be equal to the flat divisions.

$$Pec_{j+1,i} = pec_{j,i} - pec_{j,i} \quad (2)$$

The range between detected rate (the flat part) and the real rate of the peculiar part restores the peculiar part. For the progressive conversion iteration  $j$  and part  $i$ , the new peculiar part,  $j+1,i$  will be given by Equation 2. In the arising device form of the HAAR conversion the update step restores a flat part with the median of the flat/peculiar pair given by Equation 3.

$$Flat_{j+1,i} = (flat_{j,i} + pec_{j,i}) / 2 \quad (3)$$

The actual value of the pec  $j, i$  part has been restored by the disagreement between this part and its flat predecessor provided by Equation 4.

$$Pec_{j,i} = flat_{j,i} + pec_{j+1,i} \quad (4)$$

In Modified DWT the high frequency sub-bands are initially identified which is shown in Fig.6. Then this high frequency sub band is combined together with that of the low frequency sub band. Since the high sub band image consists of the few amount of approximate information content along with the edges, this is added along with the low sub band which consists of the overall information. By adding this high sub bandwidth low band almost all the useful information is present in the lower sub-band.

**D. Preminent Glaze Level Analysis**

The algorithm based on Contrast enhancement is presented for distant sensing images using discrete wavelet transform with preminent glaze level-based suitable radiance transfiguration. If the spatially altering radiance dispensation is not taken into consideration, then the corresponding contrast-improved portraits may have

**International Journal of Engineering Research in Electronics and Communication  
Engineering (IJERECE)  
Vol 3, Issue 10, October 2016**

radiance deformation and also lose portrait information. For minimizing these challenges, the entry image is down sampled into many layers of single preeminent glaze levels. To consume the low frequency radiant constituents, the DWT on the entry distant sensing picture is performed and then the developing glaze level using the log-median radiance in the Low-Low sub band is estimated. Since high-radiant values are more influential in the glaze part, and vice versa, the preeminent glaze at the position (g, h) is computed using Equation (6).

$$E(g,h)=\exp(1/OL \square(g,h) \in T \{ \log M(g,h)+\square \} ) \quad (6)$$

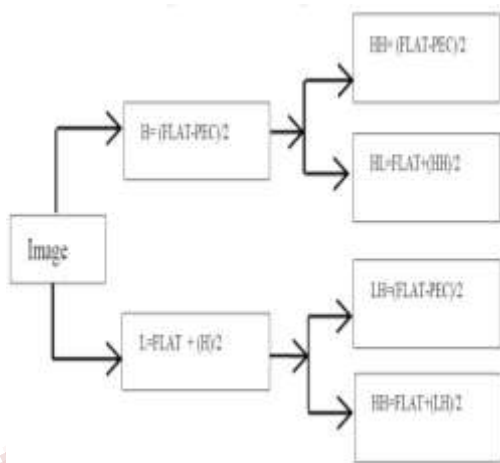


**Fig.7. Block Diagram of Modified DWT**

**III PROPOSED DUAL-TREE COMPLEX WAVELET TRANSFORM**

The decimated DWT has been widely used for performing image resolution enhancement . A common assumption of DWT-based image resolution enhancement is that the low-resolution (LR) image is the low-pass-filtered sub band of the wavelet-transformed high-resolution (HR) image. This type of approach requires the estimation of wavelet coefficients in sub bands containing high-pass spatial frequency information in order to estimate the HR image from the LR image. In order to estimate the high-pass spatial frequency information, many different approaches have been introduced. In [3] and [4], only the high-pass coefficients with significant magnitudes are estimated as the evolution of the wavelet coefficients among the scales.

The decimated DWT is not shift invariant, and as a result, suppression of wavelet coefficients introduces

artifacts into the image which manifest as ringing in the neighborhood of discontinuities. In order to combat this drawback in DWT-based image resolution enhancement, a cycle-spinning methodology was adopted in. The perceptual and objective quality of the resolution-enhanced images by their method compares favorably with that in recent methods in the field. A dual-tree complex wavelet transform (DT-CWT) is introduced to alleviate the drawbacks caused by the decimated DWT [7]. It is shift invariant and has improved directional resolution when compared with that of the decimated DWT. Such features make it suitable for image resolution enhancement. In this letter, a complex wavelet-domain image resolution enhancement algorithm based on the estimation of wavelet coefficients at HR scales is proposed. The initial estimate of the HR image is constructed by applying a cycle-spinning methodology [6] in the DT-CWT domain. It is then decomposed using the one-level DT-CWT to create a set of high-pass coefficients at the same spatial resolution of the LR image. The high-pass coefficients, together with the LR image, are used to reconstruct the HR image using inverse DT-CWT (IDT-CWT).

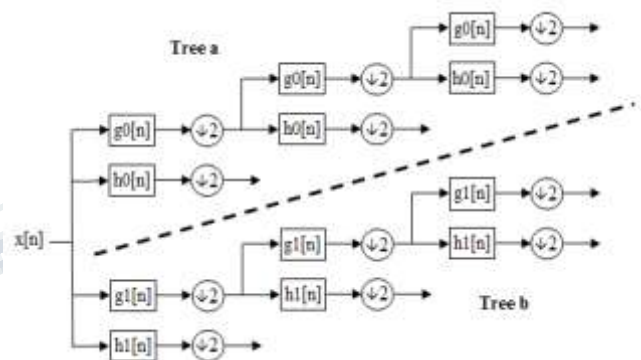


**Fig.7. Block diagram for a 3-level DTCWT**

**THE DUAL-TREE CWT** as shown in the previous section, the development of an invertible analytic wavelet transform is not as straightforward as might be initially expected. In particular, the FB structure illustrated in Figure 24 that is usually used to implement the real DWT does not lend itself to analytic wavelet transforms with desirable characteristics.

**DUAL-TREE FRAMEWORK** One effective approach for implementing an analytic wavelet transform, first introduced by Kingsbury in 1998, is called the dual-tree CWT [54], [55], [57]. Like the idea of positive/negative post-filtering of real sub band signals, the idea behind the dual-tree approach is quite simple. The dualtree CWT employs two real DWTs; the first DWT gives the real part of

**International Journal of Engineering Research in Electronics and Communication  
Engineering (IJERECE)  
Vol 3, Issue 10, October 2016**

the transform while the second DWT gives the imaginary part. The analysis and synthesis FBs used to implement the dual-tree CWT and their inverses are illustrated in Figures 7 and 8. The two real wavelet transforms use two different sets of filters, with each satisfying the PR conditions. The two sets of filters are jointly designed so that the overall transform is approximately analytic. Let  $h_0(n)$ ,  $h_1(n)$  denote the low-pass/high-pass filter pair for the upper FB, and let  $g_0(n)$ ,  $g_1(n)$  denote the low-pass/high-pass filter pair for the lower FB. We will denote the two real wavelets associated with each of the two real wavelet transforms as  $\psi_h(t)$  and  $\psi_g(t)$ . In addition to satisfying the PR conditions, the filters are designed so that the complex wavelet  $\psi(t) := \psi_h(t) + j \psi_g(t)$  is approximately analytic. Equivalently, they are designed so that  $\psi_g(t)$  is approximately the Hilbert transform of  $\psi_h(t)$  [denoted  $\psi_g(t) \approx H\{\psi_h(t)\}$ ]. Note that the filters are themselves real; no complex arithmetic is required for the implementation of the dual-tree CWT. Also note that the dual-tree CWT is not a critically sampled transform; it is two times expansive in 1-D because the total output data rate is exactly twice the input data rate. The inverse of the dual-tree CWT is as simple as the forward transform. To invert the transform, the real part and the imaginary part are each inverted—the inverse of each of the two real DWTs are used—to obtain two real signals. These two real signals are then averaged to obtain the final output. Note that the original signal  $x(n)$  can be recovered from either the real part or the imaginary part alone; however, such inverse dual-tree CWTs do not capture all the advantages an analytic wavelet transform offers. If the two real DWTs are represented by the square matrices  $F_h$  and  $F_g$ , then the dual-tree CWT can be represented by the rectangular matrix

$$F = \begin{bmatrix} F_h \\ F_g \end{bmatrix}$$

If the vector  $x$  represents a real signal, then  $wh = F_h x$  represents the real part and  $wg = F_g x$  represents the imaginary part of the dual-tree CWT. The complex coefficients are given by  $wh + jwg$ . A (left) inverse of  $F$  is then given by

$$F^{-1} = \frac{1}{2} [F_h^{-1} \quad F_g^{-1}]$$

as we can verify

$$F^{-1} \cdot F = \frac{1}{2} [F_h^{-1} \quad F_g^{-1}] \cdot \begin{bmatrix} F_h \\ F_g \end{bmatrix} = \frac{1}{2} (I + I) = I$$

We can just as well share the factor of one half between the forward and inverse transforms, to obtain

$$F := \frac{1}{\sqrt{2}} \begin{bmatrix} F_h \\ F_g \end{bmatrix}, \quad F^{-1} := \frac{1}{\sqrt{2}} [F_h^{-1} \quad F_g^{-1}]$$

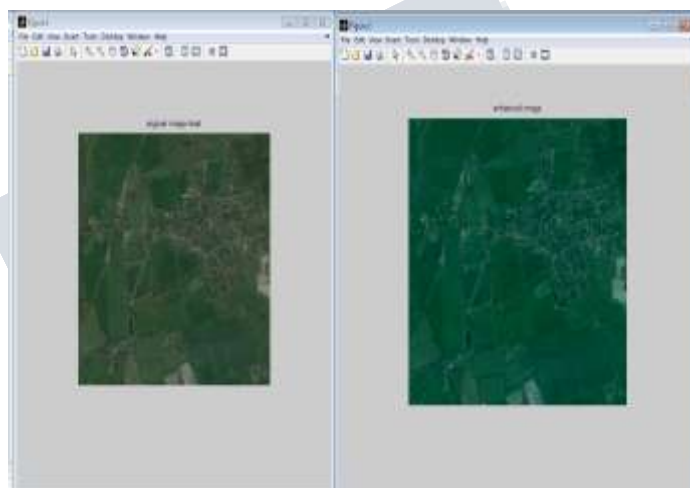


**Fig 7.DTCWT enhanced image**

**Table:1 comparison of different wavelet techniques**

METHOD	MSE	PSNR
Haar Wavelet Transform	0.9032	48.6707
Modified DWT	0.7443	49.4131
DTCWT	0.59	50.231

**CONCLUSION**

The dual-tree CWT is a valuable enhancement of the traditional real wavelet transform that is nearly shifting invariant and, in higher dimensions, directionally selective. Since the real and imaginary parts of the dual-tree CWT are, in fact, conventional real wavelet transforms, the CWT benefit from the vast theoretical, practical, and

**International Journal of Engineering Research in Electronics and Communication  
Engineering (IJERECE)  
Vol 3, Issue 10, October 2016**

---

computational resources that have been developed for the standard DWT.

#### REFERENCES

- [1] A. Abbas and T. Tran, "Fast approximations of the orthogonal dual-tree wavelet bases," in Proc. IEEE Int. Conf. Acoust., Speech, Signal Processing (ICASSP), Philadelphia, Mar. 2005, vol. 4, pp. 605–608.
- [2] A.F. Abdelnour, "Wavelet design using Gröbner bases," Ph.D. dissertation, Polytechnic Univ., Brooklyn, New York, 2003.
- [3] P. Abry, *Ondelettes et Turbulences*. Paris: Diderot, 1997.
- [4] P. Abry, S. Fauve, P. Flandrin, and C. Laroche, "Analysis of pressure fluctuations in swirling turbulent flows," *J. Physique II France*, vol. 4, no. 5, pp. 725–733, May 1994.
- [5] P. Abry and P. Flandrin, "Multiresolution transient detection," in Proc. IEEE-SP Int. Symp. Time-Frequency Time-Scale Analysis, Philadelphia, Oct. 1994, pp. 225–228.
- [6] J.-P. Antoine, R. Murenzi, and P. Vandergheynst, "Directional wavelets revisited: Cauchy wavelets and symmetry detection in patterns," *Appl. Comput. Harmon. Anal.*, vol. 6, no. 3, pp. 314–345, 1999.
- [7] J.-P. Antoine and P. Vandergheynst, "2-D Cauchy wavelets and symmetries in Images," in Proc. IEEE Int. Conf. Image Processing, Lausanne, Switzerland, Sept. 16–19, 1996, vol. 1, pp. 597–600.
- [8] H. Ates, "Modeling location information for wavelet image coding," Ph.D. dissertation, Princeton Univ., Princeton, NJ, 2003.
- [9] H.F. Ates and M.T. Orchard, "A nonlinear image representation in wavelet domain using complex signals with single quadrant spectrum," in Proc. Sailor Conf. Signals, Systems, Computers, 2003, vol. 2, pp. 1966–1970.
- [10] R.H. Bamberger and M.J.T. Smith, "A filter bank for the directional decomposition Of images: Theory and design," *IEEE Trans. Signal Processing*, vol. 40, no. 4, pp. 882–893, Apr. 1992.
- [11] B. Belzer, J.M. Lina, and J. Villasenor, "Complex, linear-phase filters for efficient image coding," *IEEE Trans. Signal Processing*, vol. 43, no. 10, pp. 2425–2427, Oct. 1995.
- [12] L. Blanc-Feraud, G.P. Bernad, and J. Zerubia, "A restoration method for confocal microscopy using complex wavelet transform," in Proc. IEEE Int. Conf. Acoust., Speech, Signal Processing (ICASSP), Philadelphia, Mar 2005, vol. 2, pp.621–624.
- [13] T.J. Burns, "A non-homogeneous wavelet multiresolution analysis and its application to the analysis of motion," Ph.D. dissertation, Air Force Inst. Technol., Ohio, 1993.
- [14] T.J. Burns, S.K. Rogers, D.W. Ruck, and M.E. Oxley, "Discrete, spatiotemporal, wavelet multiresolution analysis method for computing optical flow," *Opt. End.*, vol. 33, no. 7, pp. 2236–2247, July 1994.
- [15] E.J. Candès and D.L. Donoho, "Curvelets, multiresolution representation, and scaling laws," in Proc. Wavelet Applications Signal Image Processing VIII (Proc. SPIE), San Diego, CA, July 2000, vol. 4119, pp. 1–12.
- [16] E. Causevic, R. John, J. Kovacevic, and A. Jacquin "Adaptive complex waveletbased filtering of EEG for extraction of evoked potential responses," in Proc. IEEE Int. Conf. Acoust., Speech, Signal Processing (ICASSP), Philadelphia, Mar. 2005, vol. 5, pp. 393–396.
- [17] W. Chan, H. Choi, and R. Baraniuk, "Directional hypercomplex wavelets for Multidimensional signal analysis and processing," in Proc. IEEE Int. Conf. Acoust., Speech, Signal Processing (ICASSP), Montreal, Canada, May 2004, vol. 3, pp. 996–999.
- [18] W. Chan, H. Choi, and R. Baraniuk, "Quaternion wavelets for image analysis and processing," in Proc. IEEE Int. Conf. Image Processing, Singapore, Oct. 2004, vol. 5, pp. 3057–3060.
- [19] W. Chan, H. Choi, and R.G. Baraniuk, "Coherent image processing using quaternion wavelets," in *Wavelet Applications Signal Image Processing XI*, San Diego, CA, 2005, to be published.
- [20] J.O. Chapa and R.M. Rao, "Algorithms for designing wavelets to match a specified Signal," *IEEE Trans. Signal Processing*, vol. 48, no. 12, pp. 3395–3406, Dec. 2000.
- [21] C. Chaux, L. Duval, and J.C. Pesquet, "2D dual-tree m-band wavelet decomposition," in Proc. IEEE Int. Conf.

**International Journal of Engineering Research in Electronics and Communication  
Engineering (IJERECE)  
Vol 3, Issue 10, October 2016**

---

Acoust., Speech, Signal Processing (ICASSP), Philadelphia, Mar. 2005, vol. 4, pp. 537–540.

[22] H. Choi, J. Romberg, R.G. Baraniuk, and N. Kingsbury, “Hidden Markov tree modeling of complex wavelet transforms,” in Proc. IEEE Int. Conf. Acoust., Speech, Signal Processing (ICASSP), June 5–9, 2000, vol. 1, pp. 133–136.

[23] R.R. Coifman and D.L. Donoho, “Translation-invariant de-noising,” in Wavelets and Statistics, A. Antoniadis, Ed. New York: Springer-Verlag, 1995.

[24] M.S. Crouse, R.D. Nowak, and R.G. Baraniuk “Wavelet-based signal processing Using hidden Markov models,” IEEE Trans. Signal Processing, vol. 46, no. 4, pp. 886–902, Apr. 1998.

[25] I. Daubechies, “Orthonormal bases of compactly supported wavelets,” Com

